AGU PUBLICATIONS

JGR

Journal of Geophysical Research: Space Physics

RESEARCH ARTICLE
10.1002/2017JA023861

Special Section:
Observations, Simulations, and Theory of Electric Currents in the Solar System

Current sheets in comet 67P/Churyumov-Gerasimenko's coma

M. Volwerk[1], G. H. Jones[2,3], T. Broiles[4], J. Burch[5], C. Carr[6], A. J. Coates[2,3], E. Cupido[6], M. Delva[1], N. J. T. Edberg[7], A. Eriksson[7], C. Goetz[8], R. Goldstein[5], P. Henri[9], H. Madanian[10], H. Nilsson[11], I. Richter[8], K. Schwingenschuh[1], G. Stenberg Wieser[11], and K.-H. Glassmeier[8]

[1]Space Research Institute, Austrian Academy of Sciences, Graz, Austria, [2]Mullard Space Science Laboratory, University College London, Holmbury St. Mary, UK, [3]Centre for Planetary Sciences, UCL/Birkbeck, London, UK, [4]Space Science Institute, Boulder, Colorado, USA, [5]Southwest Research Institute, San Antonio, Texas, USA, [6]Space and Atmospheric Physics Group, Imperial College London, London, UK, [7]Swedish Institute of Space Physics, Uppsala, Sweden, [8]Institute for Geophysics and Extraterrestrial Physics, TU Braunschweig, Braunschweig, Germany, [9]Laboratoire de Physique et Chimie de l'Environnement et de l'Espace, Orleans, France, [10]Department of Physics and Astronomy, University of Kansas, Lawrence, Kansas, USA, [11]Swedish Institute of Space Physics, Kiruna, Sweden

Abstract The Rosetta Plasma Consortium (RPC) data are used to investigate the presence of current sheets in the coma of comet 67P/Churyumov-Gerasimenko. The interaction of the interplanetary magnetic field (IMF) transported by the solar wind toward the outgassing comet consists amongst others of mass loading and field line draping near the nucleus. The draped field lines lead to so-called nested draping because of the constantly changing direction of the IMF. It is shown that the draping pattern is strongly variable over the period of one month. Nested draping results in neighbouring regions with oppositely directed magnetic fields, which are separated by current sheets. Selected events on 5 and 6 June 2015 are studied, which show that there are strong rotations of the magnetic field with associated current sheets that have strengths from several tens up to hundreds of nA/m^2. Not all discussed current sheets show the characteristic peak in plasma density at the centre of the sheet, which might be related to the presence of a guide field. There is no evidence for different kinds of plasmas on either side of a current sheet, and no strongly accelerated ions have been observed which could have been an indication of magnetic reconnection in the current sheets.

Plain Language Summary The solar wind, consisting of plasma and magnetic field, cannot uninhabited flow past an active comet. The interaction of the gas coming out of the comet, which gets ionized, and the solar wind leads to a slowing down of the latter, and the magnetic field gets draped around the nucleus of the comet. As the solar wind magnetic field is not constant over time, there will be layers of different directions draped on top of each other, which leads to the generation of current sheets. In this paper the strength of the currents is determined, and signatures of possible magnetic reconnection are looked for but were not found.

Key Points:
- Magnetic field line draping pattern is highly variable over time
- Nested draping during relatively quiet solar wind times show current sheets with strengths up to hundreds of nA/m^2
- The data show no evidence that the current sheets are boundaries between different plasma regions

Correspondence to:
M. Volwerk,
martin.volwerk@oeaw.ac.at

Citation:
Volwerk, M., et al. (2017), Current sheets in comet 67P/Churyumov-Gerasimenko's coma, *J. Geophys. Res. Space Physics*, *122*, 3308–3321, doi:10.1002/2017JA023861.

Received 5 JAN 2017
Accepted 5 MAR 2017
Accepted article online 11 MAR 2017
Published online 22 MAR 2017

©2017. American Geophysical Union. All Rights Reserved.

1. Introduction

In the early view on the creation of a cometary tail by *Alfvén* [1957] (but see also *Biermann* [1952]), the solar wind magnetic field is draped around the outgassing nucleus of the comet. The solar wind magnetic field is mass loaded by local ionization of neutrals of cometary origin, which are picked up by the field lines. Conservation of momentum then implies that the mass loaded field lines should move slower than the regular solar wind speed. This requires that the magnetic field gets draped around the nucleus as the "far away" parts of the field lines are not mass loaded and continue with nominal solar wind speed, thereby stretching the field into a tail-like structure behind the nucleus as seen from the Sun.

What is missing in this simple-but-useful picture is that the solar wind magnetic field does not have a constant direction and magnitude over time. It will change due to various reasons, and this will complicate the picture, such that magnetic field of different orientations will be draped around the nucleus. Such layering of differently oriented magnetic fields near the comet is called "nested draping," which has been well observed by the Vega and Giotto spacecraft during their passage by comet 1P/Halley, as shown in Figure 4 in *Riedler et al.* [1986] and Figure 3 in *Raeder et al.* [1987], respectively, as well as in the far down-tail regions of comets

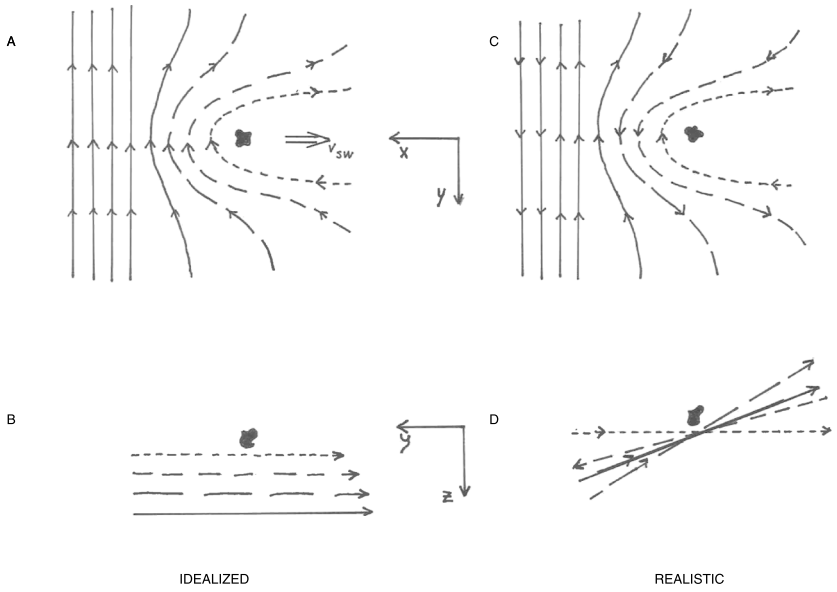


Figure 1. Magnetic field line draping around a comet for the ideal case and a more realistic case. (a) The *XY* plane for constant magnetic field being transported toward the comet by the solar wind. (b) The inner four field lines with differently dashed lines in the *YZ* plane, which should be on top of each other, but for clarity have been slightly shifted in the *z* direction. (c and d) The same view but for a more realistically behaving magnetic field which changes direction and leads to nested draping.

C/1996 B2 (Hyakutake [*Jones et al.*, 2000]) and c/2006 P1 (McNaught [*Neugebauer et al.*, 2007]). Indeed, during the complete flyby of comet 1P/Halley by the Giotto spacecraft, it was possible to identify the corresponding magnetic field directions during the inbound and outbound path.

Such magnetic field draping has also been studied extensively near comet 1P/Halley by *Israelevich et al.* [1994] and *Delva et al.* [2014]. It was found that indeed the magnetic field curves around the nucleus of the comet as expected. In a further study *Volwerk et al.* [2014] showed that there could even be an "overdraping" of the magnetic field in the region behind the terminator of the comet, similar to the draped magnetic field around Venus in the $-E_{conv}$ hemisphere [*Zhang et al.*, 2010]. Usually, the draped field lines have a parabolic shape around the object as shown in Figures 1a and 1b. However, there are occurrences that the field lines wrap around the object further behind the terminator, leading to inward/outward pointing magnetic field toward/away from the symmetry axis, i.e., the *X* axis in Figure 1. This is called overdraping.

Saturn's large moon Titan was finally encountered by Cassini in the solar wind on 13 June 2007, during which the induced magnetosphere was investigated. *Bertucci et al.* [2008] found that this magnetosphere also showed nested draping, with regions of "fossil" fields, which were related to the Kronian field, as there was a shear of over 156° between the inner field and interplanetary magnetic field (IMF) direction.

The different directions of the nested draped magnetic field lead to the creation of current sheets through Ampère's law:

$$\nabla \times \mathbf{B}(t) = \mu J(t) + \frac{\partial \mathbf{D}(t)}{\partial t}. \quad (1)$$

This situation is well known in, e.g., the Earth's magnetotail, where the cross-tail current sheet is generated by the oppositely directed magnetic fields in the northern and southern lobe [see, e.g., *McComas et al.*, 1986]. From the results by *Raeder et al.* [1987] an effort was made by *Israelevich et al.* [1994] and *Israelevich and Ershkovich* [1994] to deduce the global magnetic structure and electric currents around comet 1P/Halley, where they found currents up to tens of nA/m^2.

Interestingly, one would expect that when oppositely directed magnetic fields are pressed together in the coma around the nucleus, magnetic reconnection would take place. *Verigin et al.* [1987] observed, during a short interval, accelerated ions near comet 1P/Halley during the Vega 1 flyby, indicative of magnetic reconnection. *Kirsch et al.* [1989] studied the plasma and magnetic field data from the Giotto flyby of comet 1P/Halley

and found three different types of spikes in the particle data, one of which they posited to be related to reconnection. In a follow-up paper *Kirsch et al.* [1990] studied spikes of 5 to 15 min duration in the high-energy particle flux, which seemed to be related to regions of oppositely directed magnetic fields, including also strong changes in the pitch angles of the high-energy particles, which they considered evidence for field line merging processes.

If there is so much "nested draping" around a comet, why is there no continuous reconnection in the coma, basically peeling off the induced magnetosphere? This might be because the reconnection rate is proportional to $1/\sqrt{\rho}$, where ρ is the mass density of the plasma [see, e.g., the Sweet-Parker reconnection model *Sweet*, 1956, *Parker*, 1957] for slow and proportional to $1/\ln S$, where S is the Lundquist (or magnetic Reynolds) number, for fast reconnection [*Petschek*, 1964]. The heavy ion environment in the coma, created by the pickup of the ionized outgassing neutrals, diminishes the reconnection rate.

Lately, in the era of Rosetta [*Glassmeier et al.*, 2007a] at comet 67P/CG, currents are playing an important role in new observations. First, the so-called singing comet [*Richter et al.*, 2015] is assumed to be created by a cross-field current instability created by the freshly picked up, not yet magnetized ions around the comet. This indeed agrees with the initial observations of the motion of accelerated ions in the vicinity of the comet [*Nilsson et al.*, 2015a; *Goldstein et al.*, 2015]. *Meier et al.* [2016] discuss the possibility of the creation of the singing by a modified ion-Weibel instability [*Weibel*, 1959], generated by the cross-field current. Next to that, the discovery of the diamagnetic cavity around comet 67P/Churyumov-Gerasimenko (67P/CG) [*Goetz et al.*, 2016a] calls for a current sheet on the boundary between the magnetic and nonmagnetic regions. Using a statistical study, *Goetz et al.* [2016b] showed that there is a current sheet of up to 1 $\mu A/m^2$ on this boundary.

In this paper the draping of the magnetic field around comet 67P/CG is looked at for three flybys in the early stage of Rosetta's comet escort phase: May, June, and July 2015 (i.e., before perihelion on 13 August 2015). Only one of these three flybys, in June, shows a reasonably structured nested draping pattern, which is then studied for the occurrence of current sheets during strong rotations of the magnetic field direction.

2. Rosetta Instruments

In this paper the data from the Rosetta Plasma Consortium (RPC) instrument suite [*Carr et al.*, 2007] are used to investigate the plasma surroundings of comet 67P/CG. RPC consists of a full plasma package with a magnetometer (MAG) [*Glassmeier et al.*, 2007b], a mutual impedance probe (MIP) [*Trotignon et al.*, 2006], a Langmuir probe (LAP) [*Eriksson et al.*, 2006], an ion and electron spectrometer (IES) [*Burch et al.*, 2006], and an ion composition analyser (ICA) [*Nilsson et al.*, 2007]. All these instruments communicate with the Rosetta S/C main board computer through the plasma interface unit [*Carr et al.*, 2007].

3. Draping Around 67P/CG

During May, June, and July 2015 the Rosetta spacecraft was still in "nonbound orbits" around comet 67P/CG, because of the low gravity of and the far distance to the comet. The orbits, therefore, consisted of hyperbolic flight paths by the comet, with strong direction corrections, as can be seen in Figure 2, to maintain the so-called pyramidal orbits, which have relatively long legs of several 100 km. In this paper the data are presented in the cometocentric solar equatorial, CSEQ coordinate system (Original definition from the SPICE kernel: $+X$ axis is the position of the Sun relative to the body; it is the primary vector and points from the body to the Sun; $+Z$ axis is the component toward the Sun's north pole of date orthogonal to the $+X$ axis; $+Y$ axis completes the right-handed reference frame; the origin of this frame is the body's center of mass [*Acton*, 1996].) In order to study the draping around the comet, those parts of the orbits have been chosen which cross $Y_{CSEQ} = 0$, where in the ideal draping case the field is expected to rotate from sunward to antisunward or the other way around (depending on how the spacecraft crosses the induced magnetosphere) as shown in Figures 1a and 1b.

This ideal draping, however, does not take into account that the solar wind magnetic field is dynamic and changes direction when, e.g., a sector boundary, i.e., the heliospheric current sheet, is crossed. The changes in the field direction lead to the so-called nested draping, in which the rotations of the field are collected in the upstream pileup region at the cometary nucleus. This is schematically shown in Figures 1c and 1d.

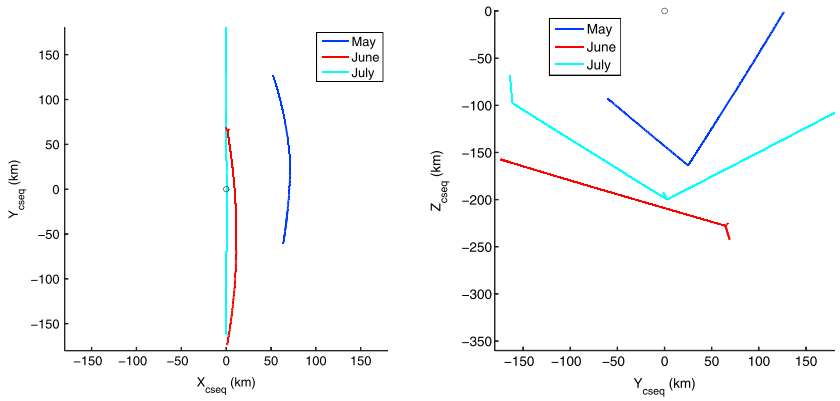


Figure 2. Three partial pyramidal orbits of Rosetta around comet 67P/CG for several days in May, June, and July in the CSEQ (left) *XY* and (right) *YZ* plane. The small circle at the origin represents comet 67P/CG.

In Figures 3a–3c the three flybys are shown with the magnetic field in the CSEQ *XY* plane, where sunward pointing magnetic field is red and antisunward pointing magnetic field is blue. Figure 3d shows the data for June in the CSEQ *YZ* plane where downward magnetic field ($B_z < 0$) is cyan and upward magnetic field ($B_z > 0$) is magenta.

The magnetic field is shown for every 300 s. It is clear that only for the June flyby (Figures 3c and 3d) there is a nicely ordered magnetic field, with mainly sunward pointing field for $Y_{CSEQ} < 0$ and mainly antisunward for $Y_{CSEQ} > 0$, resembling the original model by *Alfvén* [1957] and reminiscent of the nested draping shown by *Schwingenschuh et al.* [1987] and *Raeder et al.* [1987] around comet 1P/Halley. For May and July both directions are highly mixed. This effect can either be of solar wind origin or because of the comet-spacecraft distance during the passage or possibly spacecraft residual fields (which are smaller than 20 nT).

Recently, *Koenders et al.* [2016] used simulations of the interaction of the solar wind with the outgassing nucleus of comet 67P/CG to discuss the magnetic field draping and showed a clear event on 28 March 2015. In this case the spacecraft was mainly travelling in the *YZ* plane. Interestingly, it was found that the draping was mainly in a direction perpendicular to the solar wind flow direction, i.e., in the *Z* direction, and not, as one would expect, in the *X* direction. This is explained by the deflection of the solar wind caused by local heavy ion pickup, i.e., the acceleration of the cometary ions in the direction of the convectional electric field of the solar wind in the cometary rest frame. Because of conservation of momentum, the solar wind magnetoplasma is deflected in the direction opposite to the acceleration direction of the newly formed ions [see, e.g., *Broiles et al.*, 2015], thereby creating this unexpected field line draping direction. Indeed, a similar effect can be seen in Figure 3d, where there is also a draping signature in the *YZ* plane.

Significant deflection of the solar wind and draping was clearly seen already in the very first observations by *Nilsson et al.* [2015a], and *Broiles et al.* [2015] showed the first detailed study of the draping. Further studies showed how significant draping of the solar wind magnetic field was a clear and consistent part of the ion environment around comet 67P/CG also over longer time scales [*Goldstein et al.*, 2015; *Nilsson et al.*, 2015b]. *Behar et al.* [2016a] could even show how the deflection evolved, reaching up to nearly 90° at the end of March 2015.

4. Current Sheets in June 2015

This section will focus on possible current sheets observed on 5 and 6 June 2015. As can be seen in Figure 3, the field line draping pattern for June 2015 is reasonably well behaved; however, there are still rotations from sunward to antisunward direction and vice versa. These rotations of the magnetic field are, by necessity, associated with current sheets. Some of the rotations during 6 June 2015 were already discussed by *Volwerk et al.* [2016] on a broad scale and will now be looked at in more detail.

The magnetic field is very turbulent [see also *Richter et al.*, 2015, 2016; *Volwerk et al.*, 2016] with variations up to $\delta B/B \sim 1$ on short time scales. As the rotations of the draped magnetic field happen over a longer time scale than the turbulence, the magnetic field data are low-pass filtered using a first-order Butterworth filter with a

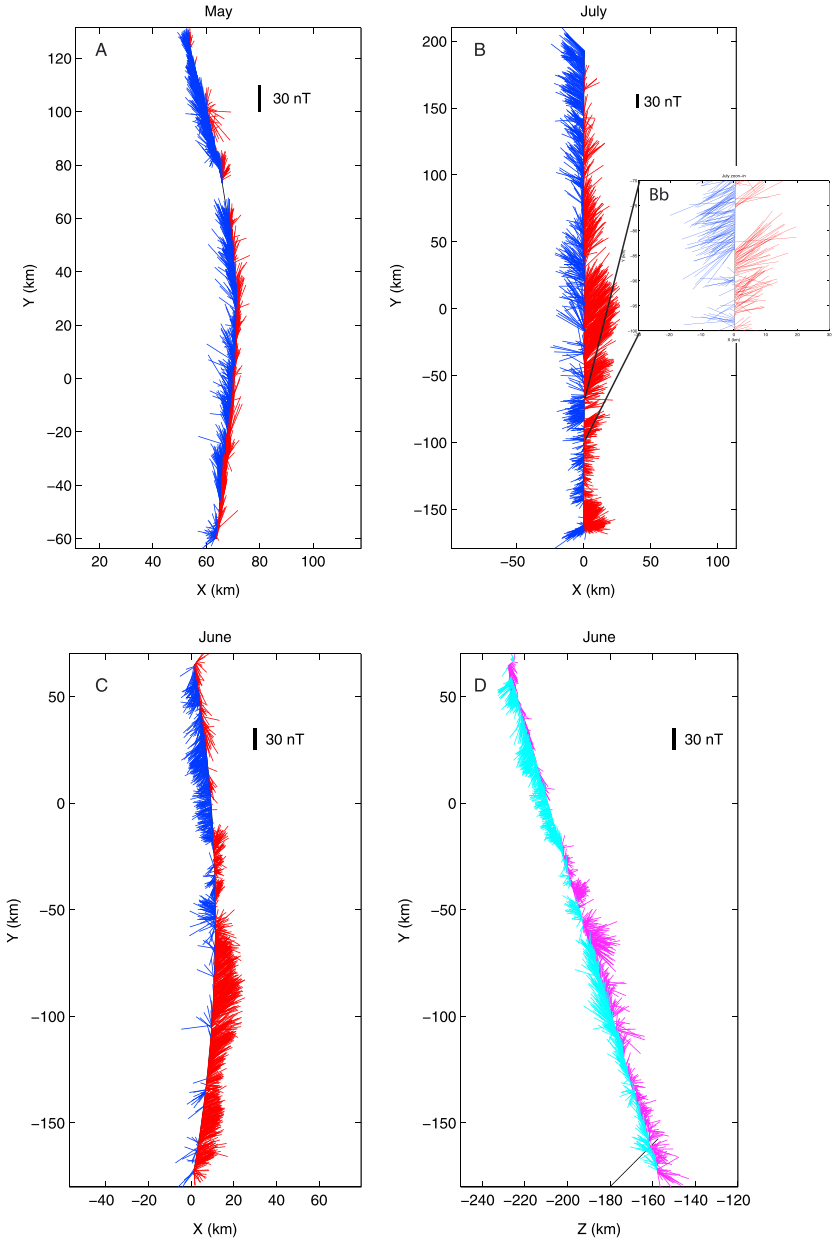


Figure 3. Hedgehog plots of the magnetic field for three subsequent flybys. (a and b) The *XY* plane for 1–8 May and 24–31 July 2015. (c and d) The *XY* and *YZ* plane for 2–9 June. For Figures 3a–3c the blue vectors show antisunward pointing magnetic field and the red vectors show sunward pointing magnetic field. For Figure 3d the cyan vectors show downward pointing magnetic field and the magenta vectors show upward pointing magnetic field. Every 300 s a vector is plotted along the orbit of Rosetta. The panels show the projected magnetic field strength onto the plane of the plot, and the black marker indicates the length of a 30 nT projected vector. Figure 3Bb shows a zoom-in of the July flyby over the interval $-100 \leq Y \leq -70$.

corner frequency of 33 mHz [*Butterworth*, 1930]. In order to find current sheets in the magnetic field data, the cone angle of the magnetic field is calculated as

$$\theta_{\text{cone}} = \tan^{-1}\left\{\frac{\sqrt{B_{\text{y,fil}}^2 + B_{\text{z,fil}}^2}}{B_{\text{x,fil}}}\right\}, \tag{2}$$

where $B_{\text{i,fil}}$ is the low-pass filtered magnetic field for component *i*. Large variations of $\theta_{\text{cone}} \geq 90°$ over relatively short time periods act as a indication for currents sheets.

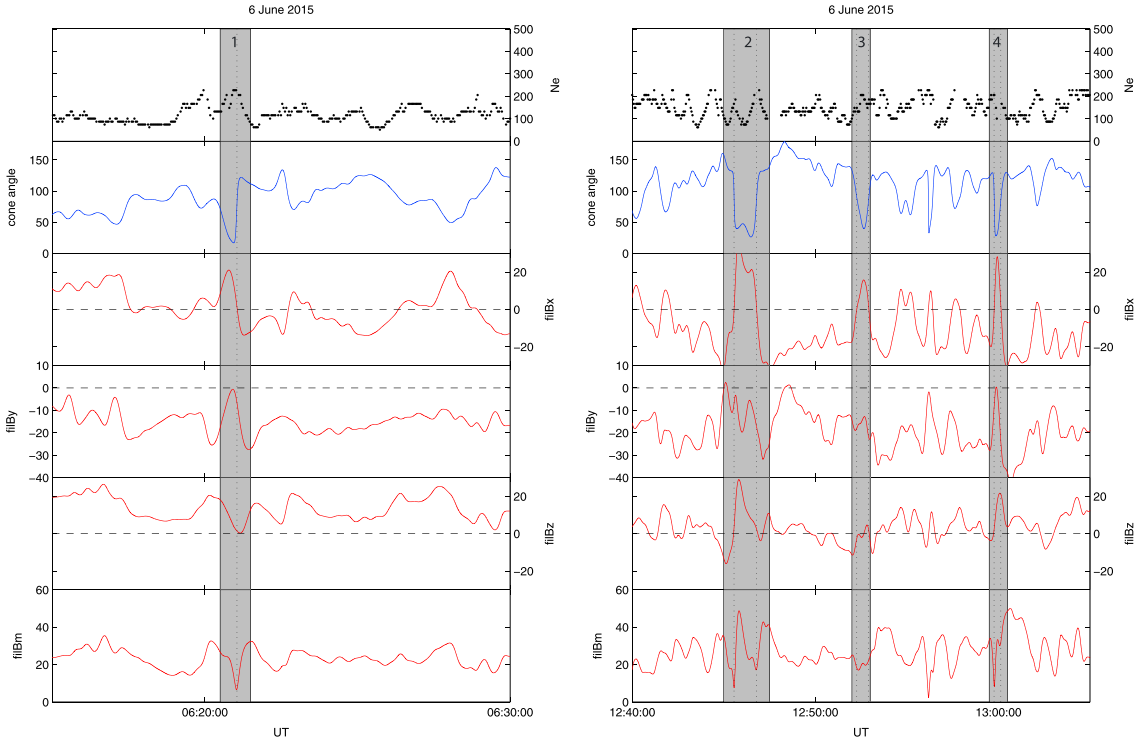


Figure 4. Current sheet events on 6 June 2015. Shown are the electron density (MIP), the cone angle, the three components, and magnitude of the low-pass filtered magnetic field. The gray boxes indicate strong fast rotations of the cone angle, and the dashed vertical lines show where $B_{x,\,fil} = 0$.

4.1. The 6 June 2015 Events

Figure 4 shows some of the events on 6 June 2015, where the gray boxes show location of large and fast cone angle changes. First, the large-scale variations of the magnetic field are studied, using the low-pass filtered magnetic field data. For a real current sheet crossing, there is a rotation of the field, the $B_{x,fil}$ changes sign, and the magnitude $B_{m,fil}$ has a minimum. Combined with this, there is a peak in the electron density. For the first event in Figure 4 (left column) a current density can be estimated using Ampère's law equation (1):

$$\nabla \times \mathbf{B} = \mu \mathbf{J} \Rightarrow J \approx \frac{\Delta B}{\mu_0 \Delta L}, \tag{3}$$

where the displacement current is neglected. With $\Delta B \approx 28$ nT and a rotation time of $\Delta t \approx 26$ s, and assuming the current sheet is convected over the spacecraft with $v \sim 10$ km/s (from IES data). Naturally, this can only be assumed when the field is frozen into the plasma, and therefore, the plasma β is estimated from the IES values. With characteristic values of $n_i \sim 50$ cm^{-3}, $T_i \sim 20,000$ K, and the magnetic field $B \sim 20$ nT, it is found that $\beta \sim 1$. This means that there can be some slippage of the field through the plasma; however, the measured IES plasma velocity will be a good estimate for the motion of the field. Thus the thickness of the current sheet is obtained through $\Delta L = v\Delta t$, and this leads to $J = 85$ nA/m^2. The current values for all events on 6 June are given in Table 1.

4.2. The 5 June 2015 Event

The situation for 5 June 2015 is rather different from the events in the previous section. As can be seen in Figure 5, there are many more oscillations of the cone angle; however, the magnitude of the magnetic field $B_{m,fil}$ is significantly lower than on 6 June. With $B_{y,fil}$ and $B_{z,fil}$ close to 0, any variations of $B_{x,fil}$ will significantly influence θ_{cone}.

In Figure 5 (left column) there are strong changes in θ_{cone}, with associated variation in the electron density measured by MIP (black) and LAP (red). There is no significant $B_{x,\,fil} = 0$ crossing during this interval, only in box 2 there is a small positive-to-negative turning. In Figure 5 (right column) four strong rotations of the field are marked in boxes 3 and 4. The estimated large-scale currents are listed in Table 1.

Table 1. Intervals of Strong Magnetic Field Cone Angle, θ_{cone}, Changes[a]

	t1 (UT)	t2 (UT)	ΔB_x (nT)	B_{min} (nT)	J (nA/m^2)	N_e (cm^{-3})
			6 June 2015			
1	06:20:51	06:21:17	28	6	85	290
2a	12:45:19	12:45:40	57	7	216	300
2b	12:46:31	12:47:05	48	17	112	320
3a	12:51:58	12:52:38	28	17	56	160[b]
3b	12:52:38	12:53:03	20	22	64	220[b]
4a	12:59:35	12:59:52	28	8	131	300
4b	12:59:52	13:00:24	39	31	97	N/A
			5 June 2015			
2	11:26:10	11:26:29	6.5	3	27	470[b]
3a	11:57:19	11:58:01	20.5	4	38	430
3b	11:59:40	12:00:14	17.5	7	41	310[b]
4a	12:25:29	12:25:53	25	2	83	920 (1620)
4b	12:32:02	12:33:11	44	11	51	420

[a]Listed are the event time windows, the change in $B_{x,fil}$, and the estimated current density under the assumption that the structure moves over the spacecraft with 10 km/s.

[b]Also listed are the MIP/LAP electron densities, where this is not the local maximum of the density (Usually the MIP and LAP densities agree reasonably well. The number between brackets for 5 June #4a is the LAP electron density deviating strongly from the MIP density for this case.).

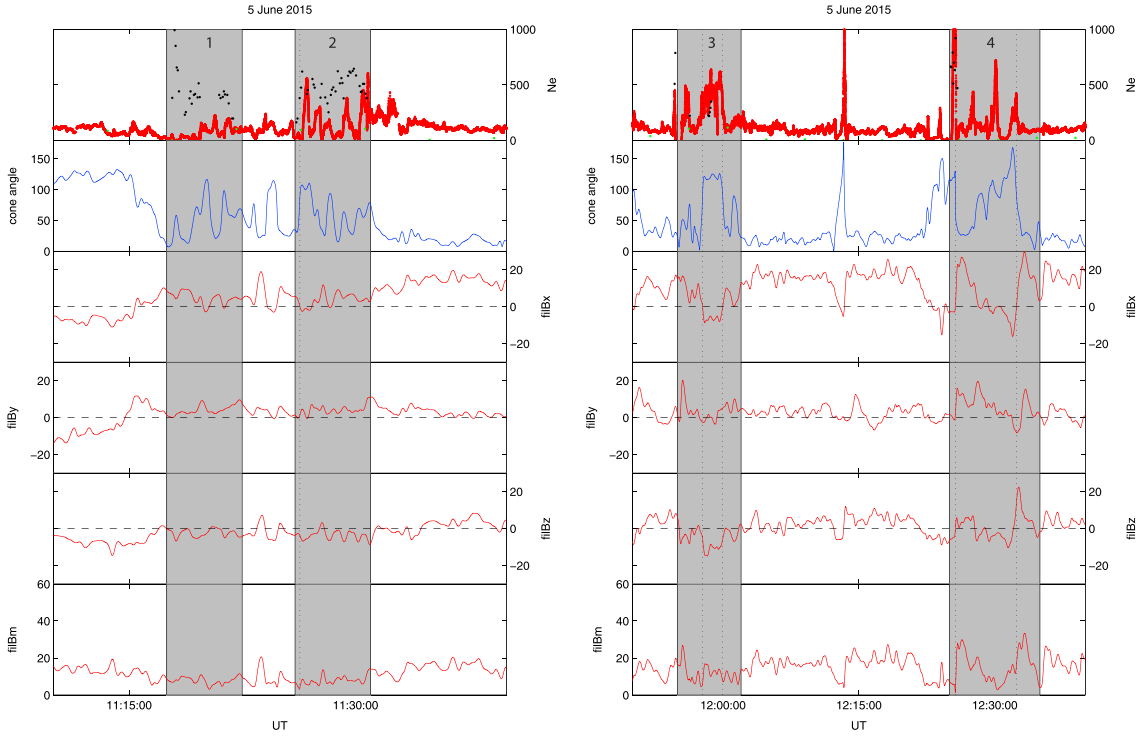


Figure 5. Current sheet events on 5 June 2015. Shown are the electron density (MIP, black dots; LAP, red dots), the cone angle, the three components, and magnitude of the low-pass filtered magnetic field and the data in magnetic field aligned coordinates. The gray boxes indicate strong fast variations of the cone angle, and the dashed vertical lines show where $B_{x,\,fil} = 0$.

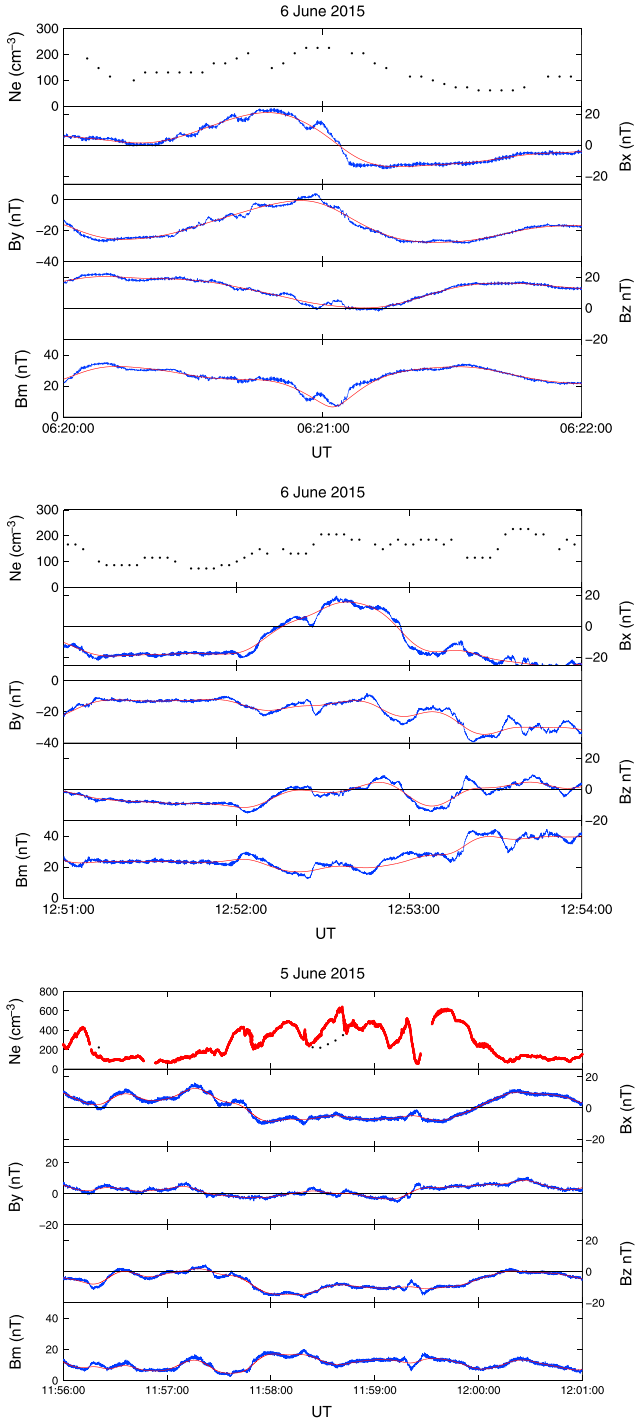


Figure 6. Three zoom-ins on magnetic field rotations. The top panels show the electron densities from MIP (black) and LAP (red, only for 5 June). The other panels show the original (20 Hz, blue) and low-pass filtered (> 30 s, red) magnetic field data. The $B_x = 0$ crossings are marked by vertical lines. It can be seen that for crossings without (or negligible) $B_{y,z}$-component the electron density peaks at the crossing, in other cases there is no maximum.

5. Electron Densities

One of the characteristics of the kind of current sheets, discussed in this paper, is that the ion and electron density increases inside the sheet while the magnetic field strength decreases, like in the current sheet of the Earth's magnetotail [see, e.g., *Harris*, 1962; *McComas et al.*, 1986; *Runov et al.*, 2005]. In Figures 4 (left panel) and 5 (left panel) the electron density as measured by MIP (black dots) and LAP (red dots) are shown. For the electron density estimates on 5 June, the LAP and MIP instruments complement each other. In the mode used here, MIP has a lower plasma density threshold of about 200 cm^{-3}, so no MIP data are available at lower densities. For LAP the limiting factor is the spacecraft potential. When this is very negative, LAP cannot access the full electron distribution, and so it underestimates the plasma density. As the spacecraft potential grows more negative when the plasma density increases [*Odelstad et al.*, 2015], the LAP density underestimate is most severe precisely when MIP densities exist and are highest, as can be seen in Figure 5 (left column). It is therefore reasonable to adapt the MIP density values when available, and the LAP estimates in the low-density intervals where MIP data are unavailable.

There is a clear correlation between the peaks in the electron density and the current sheet crossings. Indeed, every large change in θ_{cone} is accompanied by a peak in N_e, even without the "necessity" of $B_{x,fil}$ changing sign, as indicated by the data on 5 June.

In Table 1 some electron densities are found in footnote b, which indicates that this is the value of N_e at the center of the current sheet; however, it is not the local maximum density. For event 3 on 6 June, for example, the electron density peaks between the two dashed lines indicating the fast changes in θ_{cone}. This means that according to the electron density, there are two kinds of variations in the magnetic field.

Studying the various events, this seems to be related to the relative depth of the minimum in $B_{m,fil}$ during the rotation. In Table 1 the minimum field strength B_{min} at the time of $B_{x,fil} = 0$ is listed. There seems to be a

tendency that for strong rotations accompanied by a significant "guide field" (i.e., a nonzero B_y or B_z component) [see also *Yoon and Lui*, 2008], the electron density does not peak at $B_{x,fil} = 0$.

6. Nonfiltered Data

In order to see whether the low-pass filtering is causing the different behaviour of the electron density, Figure 6 shows two events on 6 June (#1 and #3 in Figure 4) and one on 5 June (#3 in Figure 5) . The original magnetic field data are in blue and the low-pass filtered data are in red. It is clear that the red curve is a reasonably good approximation, however misses, due to its construction, the higher frequency structures. This means that the $B_x = 0$ crossing actually happens faster for Figure 6 (top panel), which would lead to a higher current density than listed in Table 1. Figure 5 (first row) shows the MIP-deduced densities in black dots and the LAP densities in red (only for 5 June).

The data show that the rather large value of B_y during the $B_x = 0$ crossing in Figure 6 (middle panel) is the only significant difference between the two events. There are no "high-frequency" signatures which might invalidate using the filtered data to determine the current sheet crossing.

The event on 5 June (Figure 6, bottom panel) shows that two close rotations of the magnetic field direction can be very different. The first just before 1158 UT has a peak at the $B_x = 0$ crossing, whereas a few minutes later, at 1200 UT the rotation back to positive B_x does not show a peak in N_e. Most likely this is cause by the behaviour of B_z which after being almost zero starts to increase in magnitude at the first rotation and after having been strongly negative starts to become zero again after the second rotation.

7. Propagated Solar Wind

As there is, unfortunately, no upstream solar wind monitor at comet 67P/CG, propagation models for the solar wind are used to estimate the local conditions. Therefore, the OMNI database is used as a starting point, and the solar wind parameters are traced back from the Earth's bow shock toward the Sun and then back outward again toward comet 67P/CG, where it is assumed that the solar wind does not change during the rotation in order to reach the starting point on the surface of the Sun to reach the comet. In Figure 7 the propagated solar wind from the so-called Tao model is shown [*Tao et al.*, 2005].

Clearly, comet 67P/CG is encountering many fast solar wind conditions during the 3 month interval from May to July 2015. The dashed lines in Figure 7 show the intervals for which the draping was shown in Figure 3. Clearly, the May flyby is greatly influenced by the fast solar wind and a strong signature in B_t. The June interval shows slowing solar wind from $\sim$400 to $\sim$300 km/s with some variations in B_t. The July interval is hampered by a data gap over almost the whole period (between the two black square markers), but it shows that the solar wind changes drastically in velocity over the data gap. Quite possibly, this means that a nice draping pattern, as observed during the June interval, mainly happens when the solar wind is relatively constant or only slowly varying.

8. Nested Draping

Nested draping, i.e., the layering of differently directed magnetic field draped around the comet because of the changing solar wind conditions, was shown in various other studies near comets as mentioned in section 1. In this paper three intervals during May, June, and July 2015 have been investigated for nested draping and associated current sheets. For this effect, it is expected that the magnetic vector changes direction significantly between neighbouring regions. This can be well observed in Figure 3c, where the ideal draping directions for steady solar wind with constant magnetic field direction (like in Figure 1a) sunward for $Y \leq 0$ (red) and antisunward for $Y \geq 0$ (blue) are disturbed by regions of oppositely directed field. In the case of June the direction switch seems to be offset by ~ -20 km in Y from the comet-Sun axis.

For May and July the situation is much more complicated, as there seems to be a constant mix of red and blue vectors along the orbits. Figure 3Bb displays a zoom-in on a short interval of the July data for $-100 \leq Y_{CSEQ} \leq -70$. It shows that there are clear boundaries between Sunward and antisunward directed magnetic field intervals, and also here nested draping is an important factor in the buildup of the comet's induced magnetosphere. The different regions in Figure 3Bb are on the order of 1 h duration.

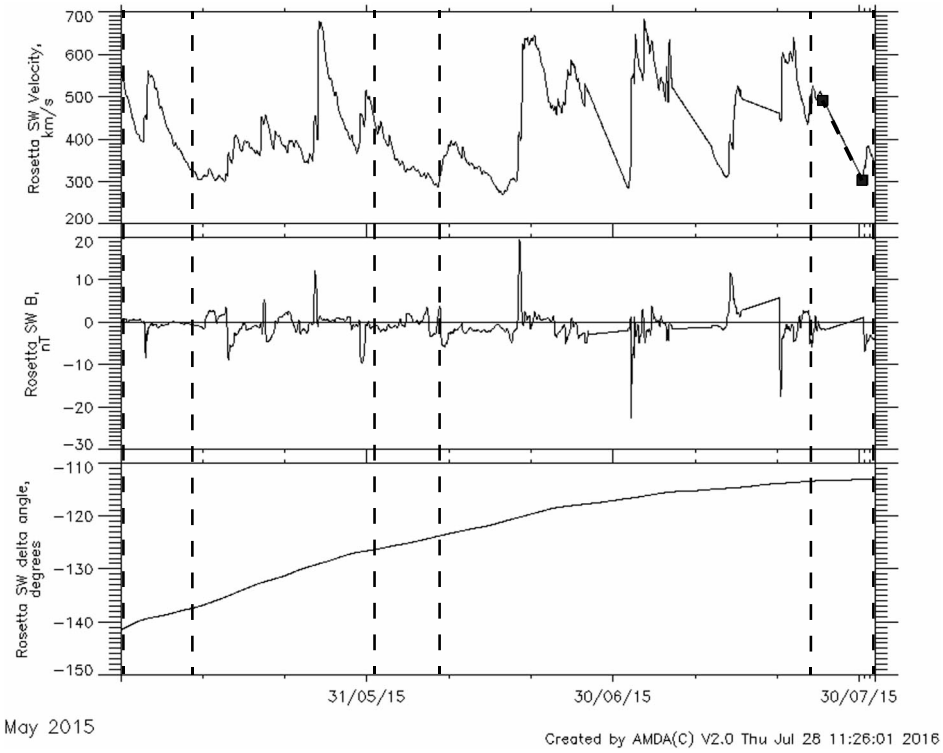


Figure 7. Propagated solar wind parameters using the so-called Tao model [*Tao et al.*, 2005]. Shown are (top) the radial solar wind velocity, (middle) the tangential magnetic field, and (bottom) the angle between the location of Earth and Rosetta. The dashed vertical lines show the intervals that are discussed in the draping section: 1–8 May, 2–9 June, and 24–31 July. The two black squares in Figure 7 (top) show the location of a data gap in the July interval.

9. Are Current Sheets Boundaries?

Nested draping around a cometary nucleus could, in principle, means that the current sheets observed between the different regions are boundaries between different kinds of plasma populations. The region where Rosetta is making measurements is totally dominated by pickup ions, and no solar wind ions are measured since the beginning of May 2015 [*Behar et al.*, 2016b]. However, the change in solar wind magnetic field direction will lead to a change in the convective electric field that the freshly created ions will experience. This can cause a difference in the plasma population if the rotation of the magnetic field is significant. In order to investigate this possibility, one of the field rotations, on 5 June 2015 #4a is studied for which both IES and ICA data are available, shown in Figure 8. The IES data are shown for 30 and 151 eV electrons, with count rate on a grid of anodes and elevations [see also *Madanian et al.*, 2016], whereas the ICA data are shown in sector plots for ions with all 96 energy steps in the top and a zoom-in to the first 48 energy steps in the bottom [see also *Nilsson et al.*, 2015a]. Four locations around the field rotation are chosen as shown by the black line in the MAG data.

It can be seen in the IES electron data that for low- and high-energy electrons just before Figure 8a, at Figure 8b, and just after Figure 8c the field rotation there is basically no difference in electron population, only later (Figure 8d) after another current sheet crossing are the electron count slightly higher than in the first three. For the ICA ions there is a slight increase in cold ion intensity near the current sheet (Figure 8b), but the accelerated ions and the cold ions are coming from the same direction in neighbouring scans (Figure 8a and 8d). This means that as far as can be measured by the RPC plasma instruments, there is no difference between the regions on either side of a current sheet. Naturally, this can easily be a result of large gyroradii of the freshly picked up ions. With a field strength of ~20 nT and an outflow velocity of the neutrals of 1 km/s, the gyroradius for water ions would be $\rho_{H_2O} \approx 9000$ km and even larger if the magnetic field is also moving toward the comet. This means that there can be ample mixing of the two plasma populations at either side of the current sheet. There are also no indications of strongly accelerated ions which might have been related to magnetic reconnection outflow.

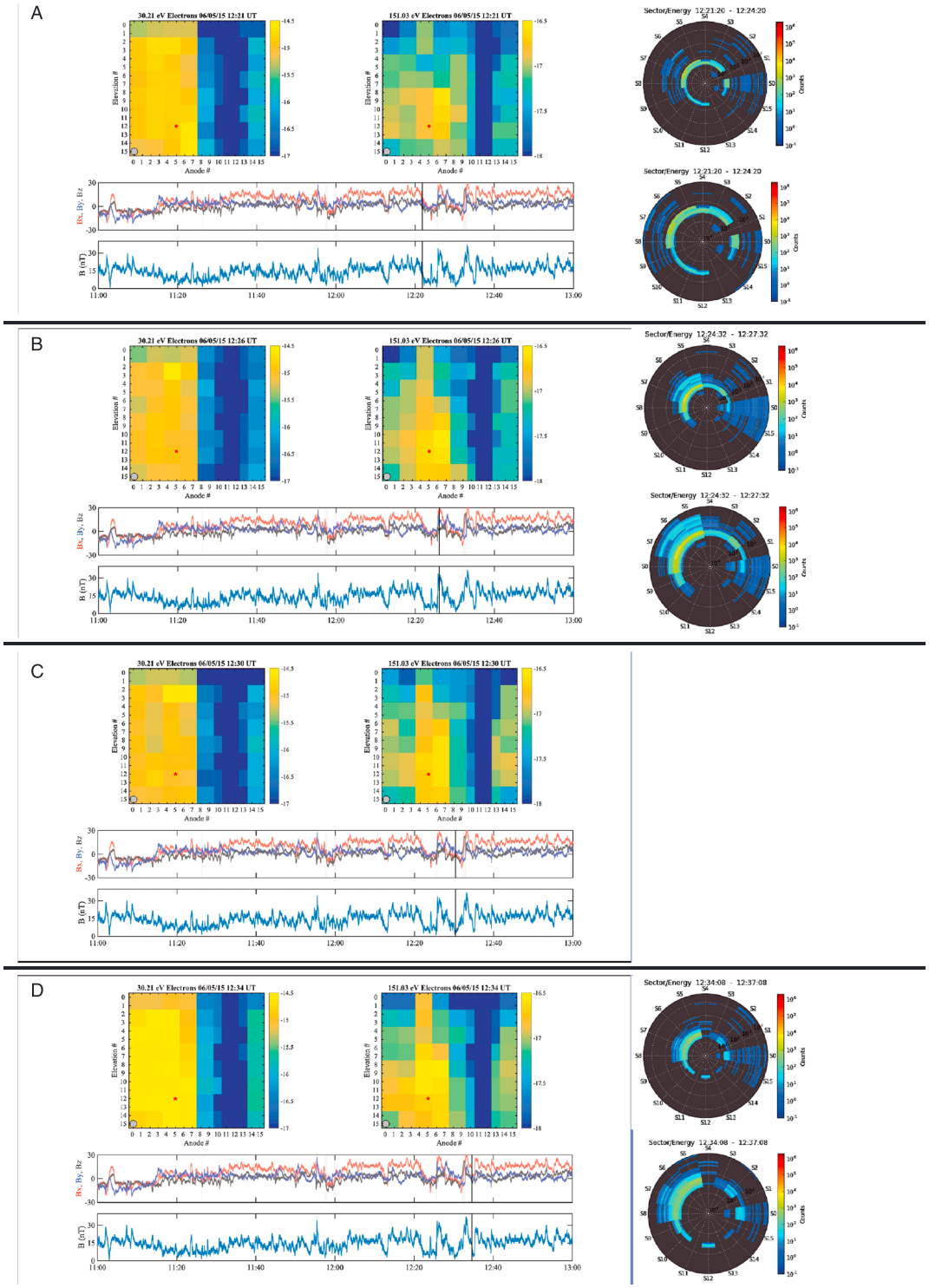


Figure 8. IES, ICA, and MAG data for four times on 5 June 2015 around field rotation #4a. Shown are the (a–d) IES electron data for 30.21 eV (top left panels) and 151.03 eV (top right panels), where the counts are plotted in an anode-elevation grid. The circle shows the direction of the comet, and the red star shows the direction of the Sun. The two panels below show the magnetic field components, and the magnitude and the rotations are marked by gray boxes. The times at which the electron data are taken is marked by a vertical black line. The right-hand panels show the ICA ion data in sector plots, where the top panel shows all 96 energy levels and the bottom a zoom-in on the first 48 levels.

10. Discussion

Magnetic field line (nested) draping has been investigated for 3 months in the early mission of Rosetta near comet 67P/Churyumov-Gerasimenko in preperihelion. It is clear from the three flybys (or partial "pyramidic" orbits) in May, June, and July 2015 that the draping pattern of the magnetic field is highly variable over the period of 1 month. Indeed, something similar over a shorter time period was also found by *Volwerk et al.* [2014] at comet 1P/Halley, comparing Vega 1 and Vega 2, and Giotto data, where the draping pattern significantly changed over a period of 8 days.

It is not clear what causes the changes in the draping pattern from very disturbed to relatively regularly draped and vice versa, whether external changes in the solar wind magnetic field are responsible or possibly the internal structure of the coma, as the flybys were at quite different locations (see Figure 2). Looking at the propagated solar wind, it is found that the two disturbed intervals (May and July) happen when there are large variations in the radial solar wind velocity, where the comet moves from a region of slow solar wind into a region of fast solar wind. The draping in June, however, happens during a period when the comet is in a region of slow solar wind and the radial velocity only slowly decreases.

Changes in the solar wind are ubiquitous in interplanetary space, so it should not be surprising to find that the events discussed in this paper are also showing strongly varying IMF conditions [see also *Edberg et al.*, 2016a, 2016b]. A study of interplanetary discontinuities was performed by *Tsurutani et al.* [1996], where a discontinuity is selected using two different criteria: first, there must be a field direction change $\Delta\mathbf{B}/|\mathbf{B}| > 0.5$ and $|\Delta\mathbf{B}| > 2\sigma$ where σ is the standard deviation at either side of the discontinuity [*Tsurutani and Smith*, 1979] and second, a directional change $\theta = \cos^{-1}(\mathbf{B}_1 \cdot \mathbf{B}_2)/|\mathbf{B}_1||\mathbf{B}_2| \geq 30°$ where $\mathbf{B}_1$ and $\mathbf{B}_2$ are vectors upstream and downstream of the discontinuity [*Lepping and Behannon*, 1986]. This selection was performed on 1 min average magnetic field data and at vectors 2 min apart, whereby the first criterion is less stringent than the second. It was found that the rate of occurrence of interplanetary discontinuities in the equatorial plane decreases with radial distance r from the Sun as $N_1 = 38\exp\{-(r-1)/5\}$ and $N_2 = 17\exp\{-(r-1)/4\}$ for $1 \leq r \leq 5$ AU.

In order to study the nested draping and associated current sheets in the cometary coma, the relatively "well behaved" data from June 2015 were used. Strong variations in the magnetic field cone angle were found, and the electron density was checked, as it is expected that the density maximizes in the middle of the rotation where the magnetic field is smallest.

1. *Currents*. The obtained current density values in Table 1 are significantly higher than the first estimate by *Volwerk et al.* [2016]. However, they are lower than the estimated current on the diamagnetic cavity, which is estimated as ~ 1 μA/m^2 *Goetz et al.* [2016b]. *Israelevich and Ershkovich* [1994] determined current densities of up to 25 nA/m^2 at comet 1P/Halley from the Giotto flyby, albeit not separated by field rotations.
   In order to check whether the estimated current densities are feasible, the MIP/LAP densities of hundreds per cubic centimeter and an estimate for the electron velocity by IES of hundreds of kilometers per second one can expect a possible maximum current density of several μA/m^2. This means that the current density estimates as listed in Table 1 are at least reasonable in the sense that they are well below this upper limit.
2. *Maximum electron density*. The location of the maximum electron density should be located in the middle of the magnetic field rotation. However, there are several events in this paper where this is not the case. For the events where the density is found in footnote b in Table 1 the maximum does not coincide with the $B_x = 0$ crossing. So, what is different about 6 June #3 and 5 June #2 and #3b? The thing to notice is that for these events, the magnetic field magnitude B_m changes less and there seems to be a "guide field" (B_y and/or B_z) present. In an ideal current sheet it tends toward $B_m = 0$ as, e.g., in 6 June #2a and to a lesser extend #2b, and also in 5 June event #3a.

11. Conclusions

This first study of current sheets in the coma of 67P/CG shows that strong rotations of the draped magnetic field occur that are similar to those observed during earlier missions at comet 1P/Halley. A relatively quiet solar wind period during of one of the early pyramidal orbits, 2–9 June, showed reasonably "well behaved" nested draping with some rotations of the field direction from sunward to antisunward and vice versa. The estimated current densities during the rotations are below that determined for the boundary of the diamagnetic cavity and below estimates for the maximum using measured electron densities and velocities. Rotations with a

strong "guide field" do not show a electron density peak near $B_x = 0$, whereas "regular" rotations, where $B_m \to 0$ show a centrally peaking density. The current sheets cannot be considered boundaries between different plasma populations, and there is no indication of accelerated ions generated by magnetic reconnection.

Acknowledgments
Rosetta is an ESA mission with contributions from its Member States and NASA. We acknowledge the staff of CDDP and IC for the use of AMDA and the RPC Quicklook database (provided by a collaboration between the Centre de Données de la Physique des Plasmas, supported by CNRS, CNES, Observatoire de Paris, and Université Paul Sabatier, Toulouse, and Imperial College London, supported by the UK Science and Technology Facilities Council). The work of K.-H. Glassmeier, I. Richter, and C. Götz was financially supported by the German Bundesministerium für Wirtschaft und Energie and the Deutsches Zentrum für Luft- und Raumfahrt under contract 50 QP 1401 for Rosetta. C. Carr and E. Cupido thank the UK Space Agency for support of the Imperial College RPC team. T. Broiles acknowledges support by NASA for work on IES through contract 1345493 with the Jet Propulsion Laboratory, California Institute of Technology. A.I. Eriksson and N.J.T. Edberg acknowledge support from the Swedish National Space Board and the Swedish Research Council. A.J. Coates and G.H. Jones acknowledge the support of the UK Science and Technology Facilities Council. Work at LPC2E/CNRS was supported by CNES and by ANR under the financial agreement ANR-15-CE31-0009-01. The Rosetta RPC data are available from ESA's Planetary Science Archive (PSA) and NASA's Planetary Data System (PDS).

References

Acton, H. C. (1996), Ancillary data services of NASA's navigation and ancillary information facility, *Planet. Space Sci.*, *44*, 65–70, doi:10.1016/0032-0633(95)00107-7.

Alfvén, H. (1957), On the theory of comet tails, *Tellus*, *9*, 92–96.

Behar, E., H. Nilsson, G. Stenberg Wieser, Z. Nemeth, T. W. Broiles, and I. Richter (2016a), Mass loading at 67P/Churyumov-Gerasimenko: A case study, *Geophys. Res. Lett.*, *43*, 1411–1418, doi:10.1002/2015GL067436.

Behar, E., J. Lindkvist, H. Nilssona, M. Holmström, G. Stenberg Wieser, R. Ramstad, and C. Götz (2016b), Mass-loading of the solar wind at 67P/Churyumov-Gerasimenko—Observations and modelling, *Astron. Astrophys.*, *596*, A42, doi:10.1051/0004-6361/201628797.

Bertucci, C., et al. (2008), The magnetic memory of Titan's ionized atmosphere, *Science*, *321*, 1475–1478, doi:10.1126/science.1159780.

Biermann, L. (1952), *Physical Processes in Comet Tails and Their Relation to Solar Activity*, pp. 251–262, La Physique des Comètes, Louvain, Belgium.

Broiles, T. W., J. L. Burch, G. Clark, C. Koenders, E. Behar, R. Goldstein, S. A. Fuselier, K. E. Mandt, P. Mokashi, and M. Samara (2015), Rosetta observations of solar wind interaction with the comet 67P/Churyumov-Gerasimenko, *Astron. Astrophys.*, A21, doi:10.1051/0004-6361/201526046.

Burch, J. L., R. Goldstein, T. E. Cravens, W. C. Gibson, R. N. Lundin, C. J. Pollock, J. D. Winningham, and D. T. Young (2006), RPC-IES: The ion and electron sensor of the Rosetta plasma consortium, *Space Sci. Rev.*, *128*, 697–712, doi:10.1007/s11214-006-9002-4.

Butterworth, S. (1930), On the theory of filter amplifiers, *Exp. Wirel. Wirel. Eng.*, *7*, 536–541.

Carr, C., et al. (2007), RPC: The Rosetta plasma consortium, *Space Sci. Rev.*, *128*, 697–712, doi:10.1007/s11214-006-9136-4.

Delva, M., C. Bertucci, K. Schwingenschuh, M. Volwerk, and N. Romanelli (2014), Magnetic pileup boundary and field draping at comet Halley, *Planet. Space Sci.*, *96*, 125–131.

Edberg, N. J. T., et al. (2016a), Solar wind interaction with comet 67P: Impacts of corotating interaction regions, *J. Geophys. Res. Space Physics*, *121*, 949–965, doi:10.1002/2015JA022147.

Edberg, N. J. T., et al. (2016b), CME impact on comet 67P/Churyumov-Gerasimenko, *Mon. Not. R. Astron. Soc.*, *462*, S45–S56, doi:10.1093/mnras/stw2112.

Eriksson, A. I. et al. (2006), RPC-LAP: The Rosetta Langmuir probe instrument, *Space Sci. Rev.*, *128*, 729–744, doi:10.1007/s11214-006-9003-3.

Glassmeier, K.-H., H. Boehnhardt, D. Koschny, E. Kührt, and I. Richter (2007a), The Rosetta mission: Flying towards the origin of the solar system, *Space Sci. Rev.*, *128*, 1–21.

Glassmeier, K.-H., et al. (2007b), RPC-MAG the flux-gate magnetometer in the ROSETTA plasma consortium, *Space Sci. Rev.*, *128*, 649–670.

Goetz, C., et al. (2016a), First detection of a diamagnetic cavity at comet 67P/Churyumov-Gerasimenko, *Astron. Astrophys.*, *588*, A24, doi:10.1051/0004-6361/201527728.

Goetz, C., et al. (2016b), Structure and evolution of the diamagnetic cavity at comet 67P/Churyumov-Gerasimenko, *Mon. Not. R. Astron. Soc.*, *462*, S459–S467, doi:10.1093/mnras/stw3148.

Goldstein, R., et al. (2015), The Rosetta Ion and Electron Sensor (IES) measurement of the development of pickup ions from comet 67P/Churyumov-Gerasimenko, *Geophys. Res. Lett.*, *42*, 3093–3099, doi:10.1002/2015GL063939.

Harris, E. G. (1962), On a plasma sheet separating regions of oppositely directed magnetic field, *Nuovo Cimento*, *23*, 115–121.

Israelevich, P. L., and A. I. Ershkovich (1994), Induced magnetosphere of comet Halley: 2. Magnetic field and electric currents, *J. Geophys. Res.*, *99*, 21,225–21,232.

Israelevich, P. L., F. M. Neubauer, and A. I. Ershkovich (1994), The induced magnetosphere of comet Halley: Interplanetary magnetic field during Giotto encounter, *J. Geophys. Res.*, *99*, 6575–6583.

Jones, G. H., A. Balogh, and T. S. Horbury (2000), Identification of comet Hyakutake's extremely long ion tail from magnetic measurements, *Nature*, *404*, 574–576.

Kirsch, E., S. McKenna-Lawlor, P. Daly, A. Korth, F. M. Neubauer, D. O'Sullivan, A. Thompson, and K. P. Wenzel (1989), Evidence for the field line reconnection process in the particle and magnetic field measurements obtained during the Giotto-Halley encounter, *Ann. Geophys.*, *7*, 107–113.

Kirsch, E., P. Daly, W.-H. Ip, S. McKenna-lawlor, and F. M. Neubauer (1990), Particle observations by EPA/EPONA during the outbound pass of Giotto from comet Halley and their relationship to large scale magnetic field irregularities, *Ann. Geophys.*, *8*, 455–462.

Koenders, C., C. Götz, I. Richter, U. Motschmann, and K.-H. Glassmeier (2016), Magnetic field pile-up and draping at intermediately active comets: Results from comet 67P/Churyumov-Gerasimenko at 2.0 AU, *Mon. Not. R. Astron. Soc.*, *462*, S235–S241, doi:10.1093/mnras/stw2480.

Lepping, R. P., and K. W. Behannon (1986), Magnetic field directional discontinuities: Characteristics between 0.46 and 1.0 AU, *J. Geophys. Res.*, *91*, 8725–8741, doi:10.1029/JA091iA08p08725.

Madanian, H., et al. (2016), Suprathermal electrons near the nucleus of comet 67P/Churyumov-Gerasimenko at 3AU: Model comparisons with Rosetta data, *J. Geophys. Res. Space Physics*, *121*, 5815–5836, doi:10.1002/2016JA022610.

McComas, D. J., C. T. Russel, R. C. Elphic, and S. J. Bame (1986), The near-Earth cross-tail current sheet: Detailed ISEE 1 and 2 case studies, *J. Geophys. Res.*, *91*, 4287–4301.

Meier, P., K.-H. Glassmeier, and U. Motschmann (2016), Modified ion-Weibel instability as a possible source of wave activity at comet 67P/Churyumov-Gerasimenko, *Ann. Geophys.*, *34*, 691–707, doi:10.5194/angeo-34-691-2016.

Neugebauer, M., et al. (2007), Encounter of the Ulysses spacecraft with the ion tail of comet McNaught, *Astrophys. J.*, *667*, 1262–1266, doi:10.1086/521019.

Nilsson, H., et al. (2007), RPC-ICA: The ion composition analyzer of the Rosetta Plasma Consortium, *Space Sci. Rev.*, *128*, 671–695, doi:10.1007/s11214-006-9031-z.

Nilsson, H., et al. (2015a), Birth of a comet magnetosphere: A spring of water ions, *Science*, *347*, aaa0571, doi:10.1126/science.aaa0571.

Nilsson, H., et al. (2015b), Evolution of the ion environment of comet 67P/Churyumov-Gerasimenko—Observations between 3.6 and 2.0 AU, *Astron. Astrophys.*, *583*, A20, doi:10.1051/0004-6361/201526142.

Odelstad, E., A. I. Eriksson, N. J. T. Edberg, F. Johansson, E. Vigren, M. André, C.-Y. Tzou, C. Carr, and E. Cupido (2015), Evolution of the plasma environment of comet 67P from spacecraft potential measurements by the Rosetta Langmuir probe instrument, *Geophys. Res. Lett.*, *42*, 10,126–10,134, doi:10.1002/2015GL066599.

Parker, E. N. (1957), Sweet's mechanism for merging magnetic fields in conducting fluids, *J. Geophys. Res.*, *62*, 509–520, doi:10.1086/146579.
Petschek, H. E. (1964), Magnetic field annihilation, in *The Physics of Solar Flares, Proceedings of the AAS-NASA Symposium held 28–30 October, 1963 at the Goddard Space Flight Center, Greenbelt, MD, NASA Spec. Publ.*, vol. 50, edited by W. N. Hess, pp. 425–439, Natl. Aeronaut. and Space Admin., Washington, D. C.
Raeder, J., F. M. Neubauer, N. F. Ness, and L. F. Burlaga (1987), Macroscopic perturbations of the IMF by P/Halley as seen by the Giotto magnetometer, *Astron. Astrophys.*, *187*, 61–64.
Richter, I., et al. (2015), Observation of a new type of low frequency waves at comet 67P/Churyumov-Gerasimenko, *Ann. Geophys.*, *33*, 1031–1036.
Richter, I., et al. (2016), Two-point observations of low-frequency waves at 67P/Churyumov-Gerasimenko during the descent of PHILAE: Comparison of RPCMAG and ROMAP, *Ann. Geophys.*, *34*, 609–622, doi:10.5194/angeo-34-609-2016.
Riedler, W., K. Schwingenschuh, Y. E. Yeroshenko, V. A. Styashkin, and C. T. Russell (1986), Magnetic field observations in comet Halley's coma, *Nature*, *321*, 288–289.
Runov, A., V. A. Sergeev, R. Nakamura, W. Baumjohann, T. L. Zhang, Y. Asano, M. Volwerk, Z. Vörös, A. Balogh, and H. Rème (2005), Reconstruction of the magnetotail current sheet structure using multi-point Cluster measurements, *Planet. Space Sci.*, *53*, 237–243.
Schwingenschuh, K., W. Riedler, Y. Yeroshenko, J. L. Philips, C. T. Russell, J. G. Luhmann, and J. A. Fedder (1987), Magnetic field draping in the comet Halley coma: Comparison of Vega observations with computer simulations, *Geophys. Res. Lett.*, *14*, 640–643.
Sweet, P. A. (1956), The neutral point theory of solar flares, paper presented at International Astronomican Union Symposium on Electromagnetic Phenomena in Cosmical Physics, p. 123, Kluwer, Dordrecht.
Tao, C., R. Kataoko, H. Fukunishi, Y. Takahashi, and T. Yokokama (2005), Magnetic field variations in the Jovian magnetotail induced by solar wind dynamic pressure enhancements, *J. Geophys. Res.*, *110*, A11208, doi:10.1029/2004JA010959.
Trotignon, J. G., et al. (2006), RPC-MIP: The mutual impedance probe of the Rosetta plasma consortium, *Space Sci. Rev.*, *128*, 713–728, doi:10.1007/s11214-006-9005-1.
Tsurutani, B. R., C. M. Ho, J. K. Arballo, E. J. Smith, B. E. Goldstein, M. Neugebauer, A. Balogh, and W. C. Feldman (1996), Interplanetary discontinuities and Alfvén waves at high heliographic latitudes: Ulysses, *J. Geophys. Res.*, *101*, 11,027–11,038, doi:10.1029/95JA03479.
Tsurutani, B. T., and E. J. Smith (1979), Interplanetary discontinuities: Temporal variations and the radial gradient from 1 to 8.5 AU, *J. Geophys. Res.*, *84*, 2773–2787, doi:10.1029/JA084iA06p02773.
Verigin, M. I., W. I. Axford, K. I. Gringauz, and A. K. Richter (1987), Acceleration of cometary plasma in the vicinity of comet Halley associated with an interplanetary magnetic field polarity change, *Geophys. Res. Lett.*, *14*, 987–990.
Volwerk, M., K.-H. Glassmeier, M. Delva, D. Schmid, C. Koenders, I. Richter, and K. Szegö (2014), A comparison between VEGA 1, 2 and Giotto flybys of comet 1P/Halley: Implications for Rosetta, *Ann. Geophys.*, *32*, 1441–1453, doi:10.5194/angeo-32-1441-2014.
Volwerk, M., et al. (2016), Mass-loading, pile-up, and mirror-mode waves at comet 67P/Churyumov-Gerasimenko, *Ann. Geophys.*, *34*, 1–15.
Weibel, E. S. (1959), Spontaneously growing transverse waves in a plasma due to an anisotropic velocity distribution, *Phys. Rev. Lett.*, *2*, 83–84, doi:10.1103/PhysRevLett.2.83.
Yoon, P. H., and A. T. Y. Lui (2008), Drift instabilities in current sheets with guide field, *Phys. Plasmas*, *15*, 072101, doi:10.1063/1.2938386.
Zhang, T. L., W. Baumjohann, J. Du, R. Nakamura, R. Jarvinen, E. Kallio, A. M. Du, M. Balikhin, J. G. Luhmann, and C. T. Russell (2010), Hemispheric asymmetry of the magnetic field wrapping pattern in the Venusian magnetotail, *Geophys. Res. Lett.*, *37*, L14202, doi:10.1029/2010GL044020.